

# Comparative studies of high performance swimming in sharks

## I. Red muscle morphometrics, vascularization and ultrastructure

D. Bernal<sup>1,\*</sup>, C. Sepulveda<sup>1</sup>, O. Mathieu-Costello<sup>2</sup> and J. B. Graham<sup>1</sup>

<sup>1</sup>Center for Marine Biotechnology and Biomedicine and Marine Biology Research Division, Scripps Institution of Oceanography, University of California San Diego, La Jolla, CA 92093-0204, USA and <sup>2</sup>Department of Medicine, University of California San Diego, La Jolla, CA 92093-0623, USA

\*Author for correspondence at present address: Department of Zoology, Weber State University, Ogden, UT 84408-2505, USA  
(e-mail: dbernal@weber.edu)

Accepted 8 May 2003

### Summary

Tunas (family Scombridae) and sharks in the family Lamnidae are highly convergent for features commonly related to efficient and high-performance (i.e. sustained, aerobic) swimming. High-performance swimming by fishes requires adaptations augmenting the delivery, transfer and utilization of O<sub>2</sub> by the red myotomal muscle (RM), which powers continuous swimming. Tuna swimming performance is enhanced by a unique anterior and centrally positioned RM (i.e. closer to the vertebral column) and by structural features (relatively small fiber diameter, high capillary density and greater myoglobin concentration) increasing O<sub>2</sub> flux from RM capillaries to the mitochondria. A study of the structural and biochemical features of the mako shark (*Isurus oxyrinchus*) RM was undertaken to enable performance-capacity comparisons of tuna and lamnid RM. Similar to tunas, mako RM is positioned centrally and more anterior in the body. Another lamnid, the salmon shark (*Lamna ditropis*), also has this RM distribution, as does the closely related common thresher shark (*Alopias vulpinus*; family Alopiidae). However, in both the leopard shark (*Triakis semifasciata*) and the blue shark (*Prionace glauca*), RM

occupies the position where it is typically found in most fishes; more posterior and along the lateral edge of the body. Comparisons among sharks in this study revealed no differences in the total RM quantity (approximately 2–3% of body mass) and, irrespective of position within the body, RM scaling is isometric in all species. Sharks thus have less RM than do tunas (4–13% of body mass). Relative to published data on other shark species, mako RM appears to have a higher capillary density, a greater capillary-to-fiber ratio and a higher myoglobin concentration. However, mako RM fiber size does not differ from that reported for other shark species and the total volume of mitochondria in mako RM is similar to that reported for other sharks and for tunas. Lamnid RM properties thus suggest a higher O<sub>2</sub> flux capacity than in other sharks; however, lamnid RM aerobic capacity appears to be less than that of tuna RM.

Key words: lamnid shark, tuna, myotome, red muscle, aerobic capacity, myoglobin, muscle ultrastructure, scaling, allometry, Lamnidae, Scombridae, *Isurus*, *Lamna*, *Alopias*, *Mustelus*, *Triakis*, *Prionace*.

### Introduction

A marked evolutionary convergence has been demonstrated for the lamnid sharks (order Lamniformes; family Lamnidae) and tunas (order Perciformes; family Scombridae) in specializations related to an increased capacity for sustained, aerobic locomotion (i.e. high-performance swimming; Bernal et al., 2001a). The sustained swimming of all fishes is powered by the red myotomal muscle (RM; Bone, 1978a) and, in most species, RM occurs along the posterior lateral edges of the body and is the dominant fiber type in that region [approximately 75–85% fork length (*FL*)] subject to maximal body bending during caudal thrust production (Greer-Walker and Pull, 1975). Lamnids and tunas, however, are different in having their RM in a more anterior and central position (Graham et al., 1983; Carey et al., 1985; Graham and Dickson, 2000, 2001; Bernal et al., 2001a).

The 'high-performance swimming adaptations' of tunas and lamnids include features enhancing tissue O<sub>2</sub> transfer at the gills (i.e. a large gill-surface area), the capacity to deliver a large quantity of O<sub>2</sub> to the RM (i.e. a large heart with a thick compact myocardial layer, a large stroke volume and well-developed coronary circulation and both a high blood hemoglobin concentration [Hb] and hematocrit) and regional endothermy (Dickson, 1996; Lai et al., 1997; Bernal et al., 2001a; Brill and Bushnell, 2001; Korsmeyer and Dewar, 2001). Although the presence of these high-performance adaptations in tunas and lamnids suggests that both groups are capable of sustaining a higher aerobic metabolism during swimming relative to that of other fishes (Bernal et al., 2001a), there is no direct experimental evidence that these adaptations increase swimming efficiency (Katz, 2002).

Relative to the RM of other fishes, tuna RM receives a large percentage of cardiac output (White et al., 1988) and has a greater capacity for mitochondrial oxidative phosphorylation (i.e. ATP production; Dickson, 1995, 1996). Consistent with the heightened aerobic capacity of tuna RM are structural and biochemical features favoring O<sub>2</sub> transfer from the RM capillaries to the fiber mitochondria. These include a relatively small RM fiber diameter, high capillary densities, the presence of capillary manifolds, which increase capillary surface area to fiber volume ratio, and a higher muscle myoglobin concentration [Mb], which enhances the diffusion of O<sub>2</sub> from the blood into the muscle cells (Wittenberg, 1970; Bone, 1978b; Mathieu-Costello et al., 1992, 1995, 1996; Dickson, 1995, 1996; Sidell, 1998; Suzuki and Imai, 1998).

The objective of this study is to provide comparative data on the position and quantity of lamnid RM and on this tissue's structural properties related to high-performance swimming. Although lamnid sharks are thought to have RM specializations for enhanced O<sub>2</sub> transfer that are comparable to those of tunas, this has not been documented. Also, data showing the position of the maximal RM cross-sectional area of makos and other lamnids presented by Carey et al. (1985) are suggestive of a tuna-like RM distribution pattern but indicate a much smaller RM quantity in lamnids relative to tunas. Using mako sharks and other lamnids, we have quantified RM position and developed an algorithm to extract more quantitative RM data from the findings of Carey et al. (1985). We also report preliminary RM ultrastructural and biochemical findings relating to lamnid RM aerobic capacity and compare these features with those of other non-lamnid sharks and tunas.

### Materials and methods

Specimens used in this study were captured, maintained and euthanized following procedures dictated by the type of study (described below) and in accordance with protocols approved by the University of California San Diego Institutional Animal Care and Use Committee.

#### *RM distribution and quantification*

The longitudinal distribution of RM was measured in two lamnid and three non-lamnid shark species. The lamnid sharks are the shortfin mako shark (*Isurus oxyrinchus* Rafinesque 1810; body mass, 5–50 kg; *N*=8) and the salmon shark (*Lamna ditropis* Hubbs and Follet 1947; 15.9–148 kg; *N*=2). The three non-lamnid sharks are the common thresher shark (*Alopias vulpinus* Bonnaterre 1788; 9.1–70.4 kg; *N*=6) and two species in the order Carcharhiniformes, the blue shark (*Prionace glauca* L.; family Carcharhinidae; 2.1–22.2 kg; *N*=4) and the leopard shark (*Triakis semifasciata* Girard 1855; family Triakidae; 1.4–15 kg; *N*=3).

In all of the species studied, measurable quantities of RM did not occur anterior to 23–25% *FL*. Beginning at this position, whole frozen sharks were cut into approximately 2–3 cm-thick transverse sections to the caudal peduncle

(85–95% *FL*). In the common thresher shark, where the RM extends far into the very long upper caudal fin lobe (Fig. 1), sections were extended to 140% *FL*.

High-resolution digital images of the anterior side of each section were obtained and the cross-sectional area of RM determined (NIH Image 4.02). For all sharks, the longitudinal distribution of RM was obtained by transforming the RM surface area (cm<sup>2</sup>) at 50% *FL* (see Table 1) to a relative value of 1 and using this value as the reference point for all other positions along the body. The volume of RM in each slice was calculated as the product of the RM surface area (mean of the anterior and posterior faces of each slice) and slice thickness. Red muscle mass in each slice was determined as the product of RM volume and RM density (predetermined to be 1.05±0.02 g cm<sup>-3</sup>, mean ± S.E.M.; *N*=10), with the sum of RM in all sections indicating total RM mass (TRMM) for the shark. Our image analysis (IA) TRMM methodology was validated for three makos (5.3 kg, 14.0 kg and 16.6 kg) by comparing TRMM results from IA with values obtained by gross dissection and gravimetric determination (GD).

The TRMM and RM linear distribution determinations for mako sharks in this study enabled us to convert the RM data presented by Carey et al. (1985) into additional estimates of TRMM. These workers had originally reported the maximal RM cross-sectional area of nine makos (5–75 kg) and expressed TRMM as a percentage of total axial muscle mass. By combining the RM data for seven of those makos with our mako RM distribution analysis, we were able to express them in terms of percentage body mass.

### *Myoglobin analysis*

#### *General*

Red muscle myoglobin concentration [Mb] was quantified using a modification of the high-performance liquid chromatography (HPLC) method of Kryvi et al. (1981). Fresh or frozen (–80°C) RM samples were obtained from *I. oxyrinchus* (5.9–46.7 kg; *N*=10), *L. ditropis* (91.2–114 kg; *N*=2) and *A. vulpinus* (6.35–45.5 kg; *N*=7). To compare our methods with those of Kryvi et al. (1981), we measured the RM [Mb] in one specimen of the gray smoothhound (*Mustelus californicus*; order Carcharhiniformes; family Triakidae; 0.8 kg), which belongs to the same order and has an RM distribution pattern similar to that of the species studied by those investigators.

Approximately 0.2 g of RM was homogenized in a 15 ml tissue grinder (Kontes Duall 23) using 9× the tissue mass of running buffer (30 mmol l<sup>-1</sup> KH<sub>2</sub>PO<sub>4</sub>, pH 7.2 at 20°C). Solid particulates were separated by centrifugation at 12 000 *g* for 10 min at 4°C and the supernatant containing the dissolved Mb was removed and diluted 2× using running buffer. Sufficient Na<sub>2</sub>S<sub>2</sub>O<sub>4</sub> (approximately 1 mg) was added to each sample supernatant to ensure that Mb was in the reduced state (cherry red in color) prior to passing the sample through a 0.45 µm syringe filter (Gelman Acrodisc LC 13 PVDF).

### HPLC parameters

Separation of tissue Mb and Hb is based on their different molecular masses (Mb, ~16 kDa; Hb, ~64 kDa) and thus their different elution times through a silica-based size exclusion column [Alltech PEEK Macrosphere GPC (60 Å; 7 µm; 4.6 mm diameter × 250 mm length), protected by a guard column (Alltech MF Guard; 60 Å; 6 µm)]. The gel permeation column (approximately 1.7 ml exclusion volume) was equilibrated with at least 150 ml of running buffer prior to the injection of the first sample. A 200 µl injection loop was used to load 25 µl of filtered and reduced tissue homogenates. Myoglobin was quantified by flowing degassed running buffer (0.3 ml min<sup>-1</sup>) through a diode array detector (Beckman Gold 168) at 413 nm.

### Myoglobin quantification

A linear relationship ( $r=0.99$ ) between known quantities of purified Mb (Sigma M 0630) and the integrated area under the curve was used to quantify RM [Mb]. The lower [Mb] detection limit was 17 pmol Mb (0.28 mg Mb g<sup>-1</sup> tissue wet mass). Verification of an adequate size-based separation was established by the injection of mixed Mb and Hb (Sigma H 4632) standards and the resulting time-separated maximum absorbance peaks.

### RM vascularization and ultrastructure

The tissues of two mako sharks (95 cm FL, 9 kg; 100 cm FL, 12 kg) were fixed *in situ* via perfusion of glutaraldehyde following methods detailed in Mathieu-Costello et al. (1992). Sharks were attracted to the boat, dip netted and returned to the laboratory alive (see Bernal et al., 2001b). Once in the laboratory, sharks were secured ventral-side up in a restraining V-board, and a 2.5 cm-diameter hose was inserted into the mouth to ensure that well-oxygenated running seawater flowed over the gills during the entire procedure. A dose of anesthetic (1:5000; MS-222) was mixed with seawater and the fish was ventilated for an additional 5–10 min to allow for complete sedation before surgery.

A midline incision exposed the heart, and a cannula was inserted into the conus arteriosus. All systemic blood returning to the heart was drained by cutting away the sinus venosus. Perfusion with heparinized saline solution [574 mmol l<sup>-1</sup> NaCl (approximately 1100 mosmol l<sup>-1</sup>) containing 20 ml l<sup>-1</sup> 1000 sodium heparin USP; Elkins-Sinn Inc., Cherry Hill, NJ, USA] preceded the fixative solution [6.25% glutaraldehyde in 0.1 mol l<sup>-1</sup> sodium cacodylate (Polysciences Inc., Warrington, PA, USA) buffer, pH 7.4 at 20°C, 132 mmol l<sup>-1</sup> NaCl (approximately 1100 mosmol l<sup>-1</sup>)]. Both the saline solution and the fixative buffer were administered at an *in vivo* non-pulsatile blood pressure of approximately 9.3 kPa (Lai et al., 1997).

Following perfusion, RM samples (1 cm×4 mm×1 mm; approximately 0.04 g) were taken at approximately 45% FL (under the first dorsal fin) and cut into longitudinal strips for storage in the fixative solution. Samples were minced into small blocks (1 mm×1 mm×2 mm) for subsequent transverse

( $\alpha=0^\circ$ , angle between normal section and muscle fiber axis) and longitudinal ( $\alpha=\pi/2$ ) section orientations and postfixed with osmium tetroxide solution prior to being embedded in Araldite for morphometric analyses using light microscopy and transmission electron microscopy, as described in Mathieu-Costello et al. (1992).

Sections (1 µm) from each mako shark were cut in transverse (4–6 blocks per shark) and longitudinal (2 blocks) orientations and stained with 0.1% aqueous Toluidine Blue solution. Morphometric analyses followed the methods in Mathieu-Costello et al. (1992) for tuna locomotor muscle. The mean sarcomere length ( $l_o$ ) in each mako was estimated from longitudinal sections by direct measurements of 40 muscle cells at 1000× magnification. A section angle closest to  $\pi/2$  was determined by rotating the tissue block on the microtome in 1° increments until the shortest  $l_o$  was measured in the sections. Mean fiber cross-sectional area [ $\bar{a}(f)$ ], and capillary density per mm<sup>2</sup> sectional area of muscle fiber [transverse,  $Q_A(0)$ ; longitudinal,  $Q_A(\pi/2)$ ] were estimated by point-counting, at 400× magnification, one transverse section from each block (total 10 blocks). Capillary density was calculated from the longitudinal sections (2 blocks) in the 9 kg mako but not in the 12 kg specimen because the capillaries were partially collapsed as a result of an incomplete perfusion fixation.

The ratio  $Q_A(0)/Q_A(\pi/2)$  was used to calculate the capillary anisotropy concentration parameter, K (from tables in Mathieu et al., 1983), and then to estimate the orientation coefficient  $c(K,0)$ , which relates the capillary counts per unit area of fiber in a transverse orientation and is used to estimate the relative increase in capillary length per volume of muscle fiber. A  $c(K,0)$  of 1 indicates that capillaries run straight and parallel to the muscle fiber axis and are unbranched, while the maximum  $c(K,0)$  value of 2 indicates that there is no preferential orientation relative to the muscle fiber axis (i.e. it is random; Mathieu et al., 1983). The product of  $Q_A(0)$  and  $c(K,0)$  was used to estimate total capillary length per volume of muscle fiber,  $J_V(c,f)$  [i.e. this term includes the contributions of capillary tortuosity (vessel convolutions that increase the fiber contact area) and branching; Mathieu-Costello et al., 1992]. The mean number of capillaries surrounding each muscle fiber ( $N_{CAF}$ ) were estimated by counting directly at a magnification of 400× ( $n \geq 200$  fibers per muscle sample), and the mean fiber diameter [ $\bar{d}(f)$ ] was estimated by  $2 \cdot [\bar{a}(f)/\pi]^{0.5}$ , assuming a circular fiber cross-sectional area. Mean capillary diameter [ $\bar{d}(c)$ ] was measured ( $n=21$ ) using a 1 µm scale eyepiece grid at a magnification of 400×. Measurement of  $\bar{d}(c)$  was limited to circle-shaped capillary sections in which the ratio between the smaller and larger diameters did not exceed 1.2 (i.e. 20%).

Mitochondrial density was measured using a total of eight tissue blocks (four from each mako) from which ultrathin (50–70 nm) transverse sections were obtained and contrasted with uranyl acetate and bismuth subnitrate (Mathieu-Costello et al., 1992). The volume densities of mitochondria and myofibrils were each measured by point-counting on 70 mm film micrographs (30–38 for each muscle sample) taken by

systematic random sampling of one transverse section from each block examined at a final magnification of 9208 $\times$  using a Zeiss 10 transmission electron microscope (Mathieu-Costello et al., 1992).

#### Statistical analysis

All statistical analyses were performed at a significance level of  $\alpha=0.05$ . The allometric relationship  $aM^{b \pm 95\% \text{ C.I.}}$  (where  $a$  is a constant and  $M$  is body mass) was used to obtain the scaling coefficient  $b$  for TRMM in the different shark species, and a

Student's  $t$ -test was used to determine if  $b=1$  (i.e. isometric scaling). The mean values for different data sets were compared using a Student's  $t$ -test.

#### Results

##### RM distribution

The linear distributions of RM in the five shark species are shown in Fig. 1. Table 1 contains the corresponding morphological data for each shark studied and data for other

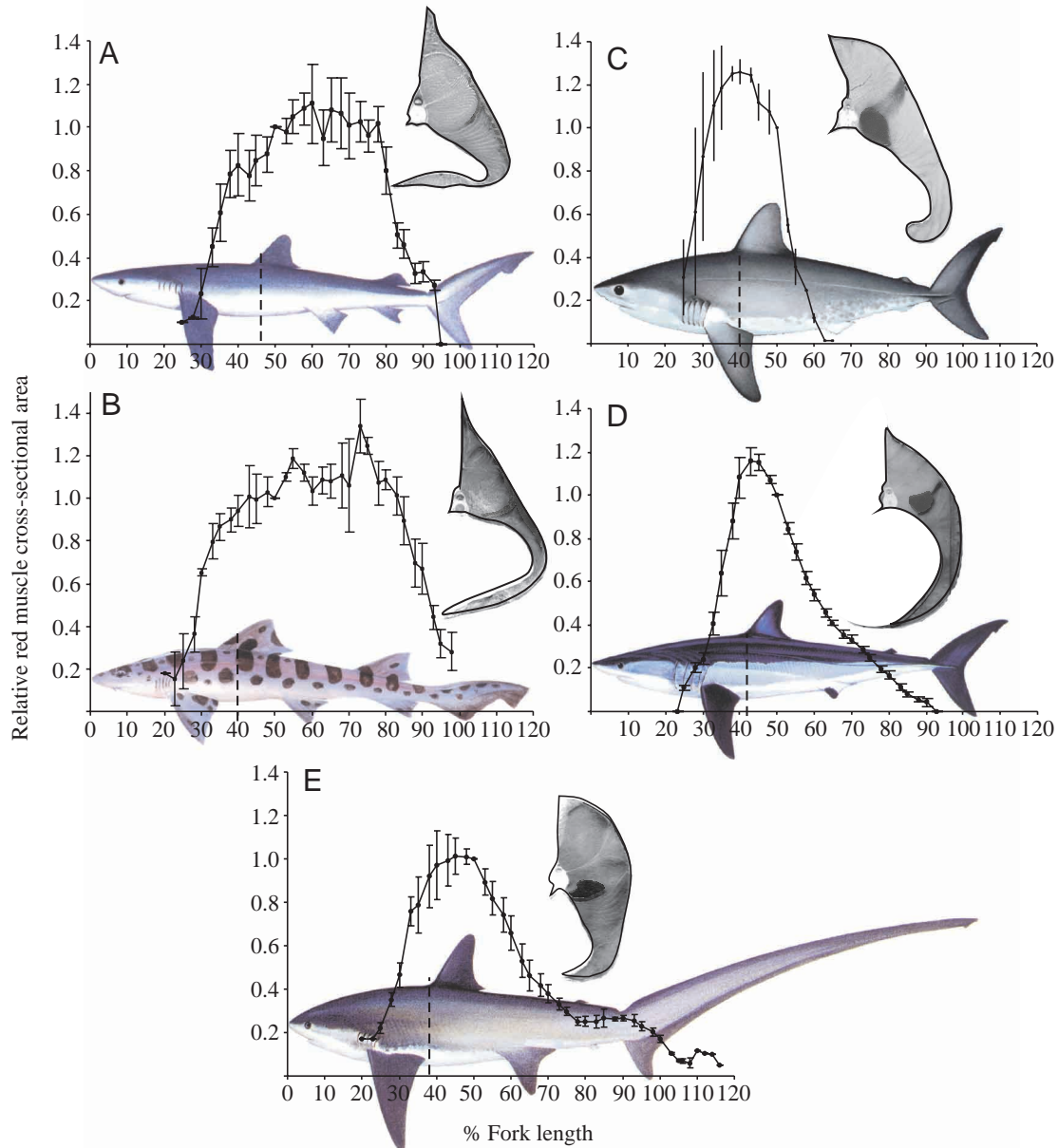


Fig. 1. Red muscle (RM) distribution patterns in five shark species. Sharks having a more posterior and lateral RM position are (A) blue shark (*Prionace glauca*) and (B) leopard shark (*Triakis semifasciata*). Sharks that have a more anterior and central RM position are (C) salmon shark (*Lamna ditropis*), (D) shortfin mako (*Isurus oxyrinchus*) and (E) common thresher shark (*Alopias vulpinus*). The relative amounts of RM in the different positions along the body are expressed as a proportion of the RM cross-sectional area equal to 1 at 50% fork length (see Table 1 for maximum surface area in cm<sup>2</sup>). Values are means  $\pm$  S.E.M., except in *L. ditropis*, where values are means  $\pm$  range. Half transverse sections of sharks showing the position of the RM (RM digitally enhanced for clarity); broken lines indicate the fork length position of the transverse section. Shark illustrations modified from Goodson (1988), Last and Stevens (1994), Allen (1997) and Tricas et al. (1997), used with permission.

Table 1. Shark red muscle (RM) body position, quantities and allometry based on data from the present study and Carey et al. (1985)

Species (common name)	RM position	Ref.	Body mass (kg)	Fork length (cm)	<i>N</i>	RM cross-sectional area at 50% <i>FL</i> (cm <sup>2</sup> )	RM mass (% of body mass)	RM scaling*
<i>Prionace glauca</i> (blue shark)	PL	a	2.1	69	4	0.69	1.05	$0.007M^{1.51\pm 0.18}$ $r^2=0.99$
			12.0	123		5.46	2.70	
			18.6	141		8.82	3.52	
			22.2	150		8.81	3.31	
						<b>Mean ± S.E.M.</b>		
						<b>2.65±0.56</b>		
<i>Triakis semifasciata</i> (leopard shark)	PL	a	1.34	52	3	0.66	1.72	$0.020M^{1.02\pm 1.51}$ $r^2=0.99$
			1.44	65		0.75	2.38	
			15.0	118		5.12	2.09	
						<b>Mean ± S.E.M.</b>		
						<b>2.06±0.19</b>		
<i>Isurus paucus</i> (longfin mako)	AC	b	–	–	–	–	~2	
<i>Isurus oxyrinchus</i> (shortfin mako)	AC	a	5.3	77	8	3.19	1.80	$0.017M^{1.07\pm 0.13}$ $r^2=0.98$
			8.6	89		6.71	1.88	
			14.0	110		7.26	1.85	
			14.3	113		10.06	2.32	
			16.6	115		10.05	2.14	
			20.6	125		9.55	2.10	
			25.8	138		11.42	1.79	
			49.9	164		18.42	2.20	
						<b>Mean ± S.E.M.</b>		
						<b>2.01±0.07</b>		
<i>Carcharodon carcharias</i> (white shark)	AC	b	5	80 <sup>†</sup>	7	4.28	2.14 <sup>‡</sup>	$0.027M^{0.91\pm 0.16}$ $r^2=0.98$
			19	123 <sup>†</sup>		10.83	2.19 <sup>‡</sup>	
			25	134 <sup>†</sup>		15.90	2.67 <sup>‡</sup>	
			33	146 <sup>†</sup>		14.83	2.06 <sup>‡</sup>	
			52	169 <sup>†</sup>		18.20	1.86 <sup>‡</sup>	
			53	170 <sup>†</sup>		17.03	1.72 <sup>‡</sup>	
			75	189 <sup>†</sup>		22.52	1.79 <sup>‡</sup>	
						<b>2.06±0.12</b>		
<i>Lamna ditropis</i> (salmon shark)	AC	a	23.6	115 <sup>§</sup>	4	6.8	~3	$0.016M^{1.15\pm 0.44}$ $r^2=0.98$
			227	235 <sup>§</sup>		54.2	~3	
			297	256 <sup>§</sup>		88.3	~3	
			1256	405 <sup>§</sup>		267.0	~6	
						<b>Mean (range)</b>		
						<b>2.09 (1.8–2.4)</b>		
<i>Lamna nasus</i> (porbeagle shark)	AC	b	–	–	1	–	~2	–
<i>Alopias vulpinus</i> (common thresher)	AC	a	4.5	85	6	5.61	2.02	$0.013M^{1.16\pm 0.35}$ $r^2=0.96$
			20.9	105		8.82	1.98	
			24.9	120		13.40	2.83	
			34.9	124		12.91	1.96	
			37.2	123		15.31	2.11	
70.4	163	35.13	3.14					
						<b>Mean ± S.E.M.</b>		
						<b>2.34±0.21</b>		

Abbreviations: a, present study; b, Carey et al. (1985); AC, anterior and central; PL, posterior and lateral.

\*Scaling equation:  $aM^{b\pm 95\%C.I.}$ , where  $a$  is a constant,  $M$  is mass (kg) and  $b$  is the scaling coefficient.

<sup>†</sup>Fork length estimated from Kohler et al. (1994).

<sup>‡</sup>Red muscle mass values estimated by using the RM longitudinal distribution analysis in Fig. 1.

<sup>§</sup>Fork length estimated from Mollet and Cailliet (1996).

lamnids, including the mako TRMM estimates derived from the original data presented by Carey et al. (1985). Lateral views of each shark together with one-half transverse sections of the body between 40% and 50% *FL* document specific differences in the lateral and linear position of RM (Fig. 1). In the blue sharks and leopard sharks, both of which have a more posterior and lateral RM position, RM is more uniformly distributed along the body (i.e. the relative cross-sectional area remains at a near maximal value between 50% and 80% *FL*), passing through the caudal peduncle and terminating at the base of the caudal fin (Fig. 1A,B). By contrast, in the lamnids and the common thresher shark, RM occurs more anterior in the body and is also in a more central position (Fig. 1C–E). The salmon shark has the most anterior RM position (peak RM area at approximately 40% *FL*) and the RM terminates far anterior of the caudal peduncle (at approximately 61% *FL*; Fig. 1C). Mako shark RM peaks slightly more posteriorly (at approximately 45% *FL*) than in the salmon shark but extends much further along the body, reaching the caudal peduncle (approximately 90% *FL*; Fig. 1D). The thresher shark has a broader region of peak RM area (45–55% *FL*) and a small quantity of RM extends as far as 140% into the upper lobe of the caudal fin (Fig. 1E).

#### RM scaling

The image analysis (IA) and gravimetric (GD) techniques for TRMM determination are in good agreement. Respective values for the three makos studied are given in terms of body mass (kg) and TRMM (kg) for IA/GD techniques: 5.3, 0.099/0.095; 14.0, 0.255/0.260; 16.6, 0.337/0.355. Table 1 shows the TRMM determined for each shark studied and also includes values for seven of the makos for which TRMM mass was estimated from the maximum RM cross-sectional area data reported by Carey et al. (1985). There is no significant difference in the RM scaling coefficients for the shark species studied and there is considerable overlap in the percentage of RM found for all species (Table 1). Moreover, the scaling coefficients and the relative amount of RM are not different, even when the shark species are separated into two distinct groups based on similarities in RM position [i.e. in a more posterior and lateral position (blue sharks and leopard sharks) vs a more anterior and central position (mako sharks, salmon sharks and common thresher sharks); Table 1]. Thus, the entire RM data set for the five species was combined to form a single scaling function ( $0.018M^{1.05\pm 0.08}$ ;  $r^2=0.96$ ,  $N=30$ ; Fig. 2). This function adequately describes RM scaling in all of the sharks studied, irrespective of the marked differences in RM position documented in Fig. 1. The scaling coefficient in this equation is not different from 1.0 (indicating isometric RM scaling) and there is no significant difference (one-way ANOVA,  $P\leq 0.05$ ) in the mean quantity of RM estimated for the different species, which ranges from 2.01% to 2.65% of body mass.

#### RM myoglobin

RM [Mb] data for seven shark species are shown in Table 2. Similarities between the Kryvi et al. (1981) [Mb] values

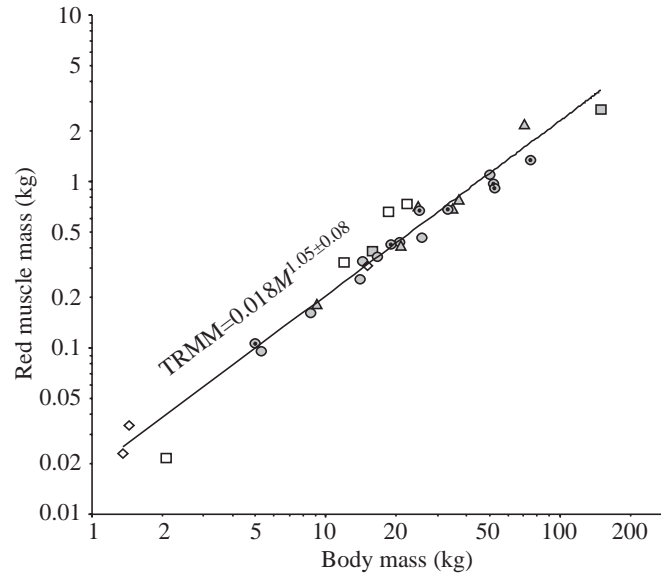


Fig. 2. Scaling of red muscle (RM) mass in five shark species. Shaded symbols represent sharks that have a more anterior and central RM position: salmon shark (squares), shortfin mako (circles); those with a dot in the middle are estimated from Carey et al., 1985) and common thresher (triangles). Unshaded symbols represent sharks that have a more posterior and lateral RM position: blue shark (squares) and leopard shark (diamonds). Species names are given in Table 1. The line defines the allometric relationship between RM mass and body mass for all sharks ( $r^2=0.96$ ,  $N=30$ ), where TRMM is total red muscle mass (kg) and  $M$  is body mass (kg).

reported for the velvet belly lantern shark (*Etmopterus spinax*; family Dalatiidae), small spotted catshark (*Scyliorhinus canicula*; family Scyliorhinidae) and blackmouth catshark (*Galeus melanopterus*; family Scyliorhinidae) and our estimates for a single gray smoothhound (7.5 mg Mb  $g^{-1}$  tissue) validate our HPLC [Mb] methodology. On the other hand, our RM [Mb] values for the salmon shark (mean, 35 mg Mb  $g^{-1}$  tissue; range 31–39 mg Mb  $g^{-1}$  tissue), shortfin mako shark (mean  $\pm$  S.E.M.,  $21\pm 2.4$  mg Mb  $g^{-1}$  tissue) and common thresher shark ( $16.3\pm 1.6$  mg Mb  $g^{-1}$  tissue) range from 3 $\times$  to 12 $\times$  higher than values reported by Kryvi et al. (1981) for sharks in Table 2 and are among the highest reported to date for any fish species (Dickson, 1996). The slopes of the scaling equations determined for both the mako and common thresher shark [Mb] per g RM tissue do not change with body mass (i.e. slopes are not significantly different from zero).

#### RM vascularization and ultrastructure

Mako RM vascularization and ultrastructure details are shown in Figs 3, 4. Table 3 provides additional morphometric data (based on a mean  $l_0$  of 2.06  $\mu m$ ) for mako RM and comparative data for other species. We found little variation in the RM ultrastructure and vascularization of the two relatively small (9.7–12 kg) makos studied. We did, however, note some collapsed capillaries and a few remaining erythrocytes (Fig. 3B,C) in some of the RM transverse blocks, which

Table 2. Myoglobin concentrations in the red muscle (RM)

Species (common name)	RM position*	Body mass (kg)	<i>N</i>	[Myoglobin] <sup>†</sup> (mg Mb g <sup>-1</sup> tissue)	Source
<b>Shark</b>					
<i>Lamna ditropis</i> (salmon shark)	AC	91–114	2	35.1 (range, 31.2–38.9)	Present study
<i>Isurus oxyrinchus</i> (shortfin mako)	AC	6–47	10	21.1±2.4	Present study
<i>Alopias vulpinus</i> (common thresher)	AC	6–46	7	16.3±1.6	Present study
<i>Mustelus californicus</i> (gray smoothhound)	PL	0.8	1	7.5	Present study
<i>Scyliorhinus canicula</i> (small spotted catshark)	PL	~0.5‡	3	9.1±1.6	Kryvi et al. (1981)
<i>Etmopterus spinax</i> (velvet belly lantern shark)	PL	~0.2‡	3	8.3±0.4	Kryvi et al. (1981)
<i>Galeus melastomus</i> (blackmouth catshark)	PL	~0.2‡	3	2.7±0.4	Kryvi et al. (1981)
<b>Tuna</b>					
<i>Thunnus albacares</i> (yellowfin tuna)	AC			31.4	Dickson (1996)
<i>Katsuwonus pelamis</i> (skipjack tuna)	AC			20.8	Dickson (1996)
<i>Thunnus orientalis</i> (Pacific northern bluefin tuna)	AC			Range, 20–24	Dickson (1996)

\*Red muscle position: anterior and central (AC) or posterior and lateral (PL).

<sup>†</sup>Except where indicated, values represent means ± S.E.M.

<sup>‡</sup>Sizes given by Kryvi et al. (1981) are 'adult specimens', and body mass is estimated from the size at sexual maturation (Froese and Pauly, 2002).

suggests an incomplete *in vivo* perfusion fixation and thus an underestimation of  $Q_A(0)$ ,  $Q_A(\pi/2)$  and  $N_{CAF}$ .

Longitudinal and transverse RM fiber sections (Fig. 3A–C) detail capillary distributions and suggest the presence of capillary manifolds. Mako RM capillary density [ $Q_A(0)=743\text{--}918\text{ mm}^{-2}$ ] appears to be the highest measured to date for any shark, ranging from 1.7× to 5.9× higher than in the other species (i.e. the blackmouth catshark and velvet belly lantern shark) and is also 7× higher than in the *Chimaera monstrosa* (rabbit fish) (Table 3). Relative to the other sharks, RM  $N_{CAF}$  is significantly higher in both the shortfin mako shark and blackmouth catshark, which are not significantly different from each other. The capillary-to-fiber ratio [ $N_N(c,f)$ ] is 1.4–10.8× greater in mako RM relative to other sharks and the rabbit fish (Table 3). Mako shark RM fiber cross-sectional area [ $\bar{a}(f)$ ;  $1437\text{ }\mu\text{m}^2$ ] is not statistically different from the values for the blackmouth catshark and rabbit fish but is smaller than in the velvet belly lantern shark (Table 3). An electron micrograph of mako RM (Fig. 4) shows the relationship between myofibrils, subsarcolemmal and intrafibrillar mitochondria and other cellular structures. The total volume density of mitochondria [ $V_V(mt,f)$ ] in mako RM (mean, 27.4%) is in the range of values given for the RM of other sharks (30.4–34.1%) and tunas (28.5%) (Table 3).

## Discussion

Our findings support the hypothesis that the lamnid shark–tuna evolutionary convergence for high-performance swimming extends to similarities in RM position and in features augmenting RM aerobic capacity.

### *RM distribution and scaling*

#### *Biomechanical implications of RM position*

Aerobically functioning RM powers the sustained swimming of most fishes. In the majority of sharks and bony fishes, RM occurs mainly in the posterior half of the body along the lateral midline, directly under the skin (Greer-Walker and Pull, 1975; Bone, 1978a; Fig. 1). RM in this position is linked mechanically to the skin as well as to the adjacent myotomal white muscle (WM). Force transmission from the RM to the caudal fin therefore occurs *via* the skin and also involves the local bending of body segments remote from the caudal fin (i.e. the bending waves seen in most fish swimming modes, including the anguilliform swimming of sharks; Lindsey, 1978; Sfakiotakis et al., 1999).

In occurring both more anterior in the body and more central (i.e. nearer the vertebral column; Fig. 1), the lamnid RM distribution (and that of the common thresher shark) is different from that of most sharks and similar to that of tunas (Graham et al., 1983; Carey et al., 1985; Bernal et al., 2001a).

Also, and in contrast to most sharks, lamnid RM is neither connected to the adjacent WM or the skin. Rather, it extends, *via* connective myocomata, directly into the thick skin of the caudal keel (Reif and Weishampel, 1986; fig. 5 in Bernal et al., 2001a). Force from the RM is thus transmitted directly to the

caudal fin and does not impose strain on either the surrounding WM or the adjacent skin.

Similarities in lamnid and tuna RM position have been postulated to reflect convergence in both body shape and the development of a more rigid swimming mode. With respect to body shape, an anterior shift in RM position reduces posterior-body height, thereby increasing both posterior-body taper and streamlining (Graham and Dickson, 2000). Biomechanical studies of skipjack tuna (*Katsuwonus pelamis*) and yellowfin tuna (*Thunnus albacares*) (Shadwick et al., 1999; Katz et al., 2001; Katz, 2002) and work in progress with the mako shark (J. Donley and R. Shadwick, personal communication) indicate that the anterior and central RM position imparts a mechanical benefit during sustained swimming. This benefit, the reduction of hydrodynamic drag through a lessening of the extent of lateral displacement of more anterior body segments during force production, is derived from the decoupling of RM contraction from local body bending (this would occur if RM fibers were connected to either the adjacent WM or skin). In other words, with a direct link between the remotely positioned RM and the caudal fin, both tunas and lamnids swim with more rigid bodies,

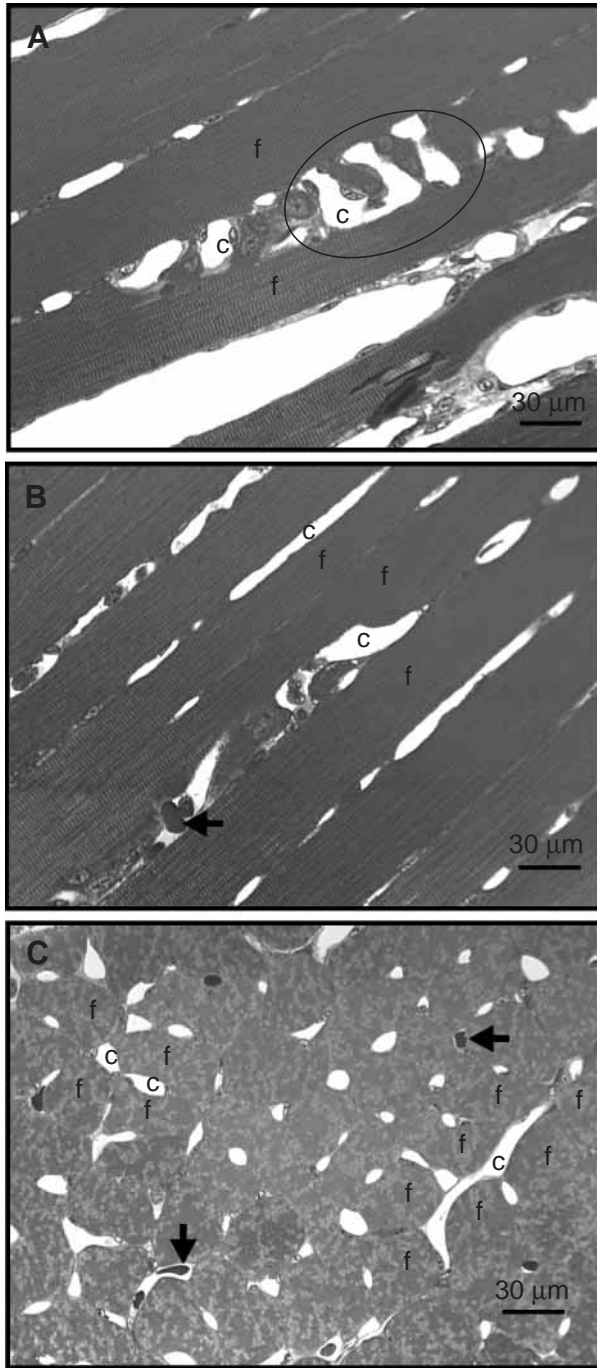


Fig. 3. Light micrographs (400 $\times$  magnification) of mako shark (9.7 kg, 95 cm fork length) red muscle (RM) in longitudinal (A,B) and transverse (C) orientations. The oval in frame A encloses a putative capillary manifold. Some capillaries (c) and fiber bundles (f) are labeled for clarity, and arrows point to some remaining erythrocytes within the capillary lumen.

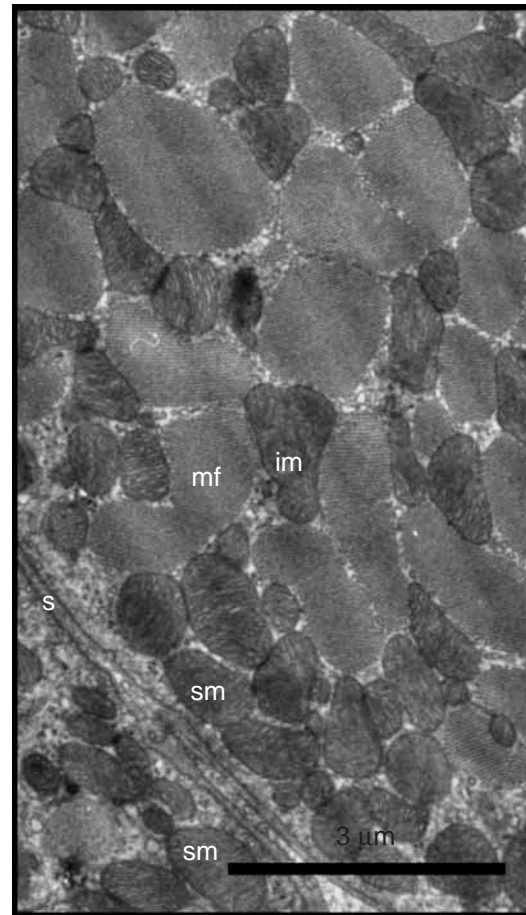


Fig. 4. Electron micrograph (9208 $\times$  magnification) of a mako shark (9.7 kg, 95 cm fork length) red muscle (RM) transverse section. Abbreviations: s, subsarcolemma; mf, myofibrils; im, interfibrillar mitochondria; sm, subsarcolemmal mitochondria.

which reduces induced drag (Shadwick et al., 1999; Altringham and Shadwick, 2001; Bernal et al., 2001a; Katz, 2002).

*RM position and endothermy*

In addition to its biomechanical importance, the central and

anterior RM position of tunas and lamnids is closely linked to another unique feature shared by these groups, the capacity to maintain elevated temperatures in RM and other tissues (regional endothermy; Carey et al., 1971; Bernal et al., 2001a,b). Endothermy increases total aerobic metabolic

Table 3. Red muscle (RM) vascularization and ultrastructure in sharks and tuna

Species (common name; N)	Mass (kg)	Fork length (cm) <i>FL</i>	Sarcomere length (μm) <i>l<sub>o</sub></i>	Capillary numerical density (mm <sup>-2</sup> )		Muscle fiber	
				<i>Q<sub>A</sub>(0)</i>	<i>Q<sub>A</sub>(π/2)</i>	Area (μm <sup>2</sup> )	Diameter* (μm)
						<i>ā(f)</i>	<i>d̄(f)</i>
<i>Isurus oxyrinchus</i> (shortfin mako shark; N=2)	9.7	95	2.04±0.01	918±59	316±28	1396±43	42.2
	12.0	100	2.07±0.01	743±67	–	1477±83	43.4
<b>Mean</b>			<b>2.055</b>	<b>831</b>	–	<b>1437</b>	<b>42.8</b>
<i>Galeus melastomus</i> (blackmouth catshark; N=7)			–	484	–	1778±308	47.6
<i>Etmopterus spinax</i> (velvet belly lantern shark; N=7)			–	141	–	2617±369	57.7
<i>Chimaera monstrosa</i> (rabbit fish; N=6)			–	118	–	954±303	34.9
<i>Katsuwonus pelamis</i> (skipjack tuna; N=8)	~2	44	1.78±0.02	2880±171	1615±114	560±30	–

Table 3. Continued

Species (common name; N)	Capillaries around fiber <i>N<sub>CAF</sub></i>	Capillary-to- fiber ratio <i>N<sub>N(c,f)</sub></i>	Capillary diameter (μm) <i>d̄(c)</i>	Anisotropy coefficient <i>c(K,0)</i>	Capillary length per fiber volume (mm <sup>-2</sup> ) <i>J<sub>V</sub>(c,f)</i>	Volume density of mitochondria (%) <i>V<sub>v</sub></i>	Volume density of myofibrils (%) <i>V<sub>v</sub>(my,f)</i>
<i>Isurus oxyrinchus</i> (shortfin mako shark; N=2)	3.74±0.07	1.28	9.4±0.5	1.19	1092.4	25.2±0.8 <sup>‡</sup> ; 21.0±0.8 <sup>‡</sup> ; 4.1±0.9 <sup>§</sup>	59.7±1.5
	3.64±0.08	1.10	6.4±0.6	–	–	29.5±1.2 <sup>‡</sup> ; 22.2±1.3 <sup>‡</sup> ; 7.2±1.9 <sup>§</sup>	52.3±1.8
<b>Mean</b>	<b>3.69</b>	<b>1.19</b>	<b>7.9</b>	–	–	<b>27.4<sup>‡</sup>; 21.6<sup>‡</sup>; 5.7<sup>§</sup></b>	<b>56</b>
<i>Galeus melastomus</i> (blackmouth catshark; N=7)	2.5±0.45	0.86	–	–	–	34.1±1.9 <sup>‡</sup>	–
<i>Etmopterus spinax</i> (velvet belly lantern shark; N=7)	1.4±0.26	0.37	–	–	–	30.4±1.8 <sup>‡</sup>	–
<i>Chimaera monstrosa</i> (rabbit fish; N=6)	0.3±0.16	0.11	–	–	–	5.2±0.9 <sup>‡</sup>	–
<i>Katsuwonus pelamis</i> (skipjack tuna; N=8)	4.97±0.13	1.59	4.0±0.3	1.44±0.04	4143±242	28.5±1.0 <sup>a,‡</sup> ; 19.7±0.6 <sup>a,‡</sup> ; 8.8±1.1 <sup>a,§</sup> ; 24–32 <sup>b,‡</sup>	66.1±0.9

All values are means ± S.E.M.

Abbreviations: *FL*, fork length; *Q<sub>A</sub>(0)*, transverse orientation; *Q<sub>A</sub>(π/2)*, longitudinal orientation.

Data for *G. melastomus*, *E. spinax* and *C. monstrosa* from Totland et al. (1981).

Data for *K. pelamis* from <sup>a</sup>Mathieu-Costello et al. (1992) and <sup>b</sup>Moyes et al. (1992).

\*Fiber diameter estimated by  $2[(\bar{a}(f)/\pi)^{0.5}]$ ; †values given are *V<sub>v</sub>(mt,f)* (total mitochondria); ‡values given are *V<sub>v</sub>(mi,f)* (interfibrillar mitochondria); §values given are *V<sub>v</sub>(ms,f)* (subsarcolemmal mitochondria).

biochemical capacity (see Bernal et al., 2003) and power output of tunas and lamnids and has also contributed to the adaptive radiation of both groups (Carey and Teal, 1966; Johnston and Brill, 1984; Dickson, 1995, 1996; Brill, 1996; Altringham and Block, 1997; Graham and Dickson, 2001). The functional basis of endothermy in both groups is the capacity of the RM vascular supply to conserve, by counter-current heat exchange, metabolic heat generated by the continuous action of the highly oxidative RM (Carey and Teal, 1966, 1969a,b; Carey et al., 1971, 1985; Anderson and Goldman, 2001; Bernal et al., 2001a,b). Although the Alopiidae resemble lamnids in having a central and anterior RM position (Fig. 1) that is served by a lateral circulation and a small putative heat exchanger (Bone and Chubb, 1983; Block and Finnerty, 1994; D. Bernal, C. Sepulveda and K. Dickson, personal observations), there are no published descriptions conclusively documenting RM endothermy in the thresher sharks (Carey et al., 1971).

#### *Interspecific differences in RM position*

Although we found the RM position of the two lamnids and the common thresher shark to be generally similar to that of tunas, there are noteworthy specific differences among the sharks (Fig. 1). In makos, RM ends at the caudal peduncle (approximately 90% *FL*). In the salmon shark, RM ends well in advance of the peduncle (approximately 61% *FL*) and, in the thresher, RM reaches far into the caudal fin's upper lobe (140% *FL*).

How might these various RM positions relate to the locomotion and biology of the different species? Assuming the RM–caudal fin linkage of the salmon shark is similar to that of the mako, a shorter RM section requires a longer force-transmitting connection between RM and the caudal fin. This would in turn imply a more rigid (less undulatory) swimming mode for the salmon shark relative to the mako. By this standard, extension of RM well into the upper caudal lobe of the common thresher's caudal fin implies greater tail flexibility (i.e. both maneuverability and mobility), which is consistent with the tail's importance in feeding (Gubanov, 1972). During feeding, we have observed the long caudal lobe of threshers being used to herd small schooling fishes (e.g. sardines and anchovies) into a tight group and then 'clubbing' and stunning the prey prior to feeding. Also, many of the thresher sharks we captured for this study were hooked by the upper lobe of the caudal tail, a capture scenario also reported by Gruber and Compagno (1981).

#### *Comparative aspects of RM scaling*

Findings for sharks in this study indicate TRMM values of 2–3% of total body mass with no interspecific differences (Table 1). Thus, neither RM position nor presumed differences (based on morphology and behavior) in high-performance swimming capacity (i.e. lamnids vs less mobile forms) correlate with TRMM.

This contrasts with what is known for tunas, in which TRMM ranges from 4% to 13% of total body mass (Graham et al., 1983). While the relative amount of RM in some tuna

species is higher than in any other fish species (e.g. black skipjack tuna *Euthynnus lineatus* 11%; frigate tuna *Auxis thazard* 13%), the TRMM of most tunas is similar to values for other fishes (Graham et al., 1983; Graham and Dickson, 2000, 2001). Furthermore, comparisons within the family Scombridae show that the scaling coefficient for tuna RM is less than or equal to 1.0, while the RM scaling coefficient for non-tunas is significantly greater than 1.0 (Graham et al., 1983; Goolish, 1989). Thus, while tuna TRMM is directly proportional to body size, or even declines with size in some tuna species, TRMM in non-tuna scombrids increases at a disproportionately greater rate than body size.

The RM scaling coefficient determined for lamnids in this study is not different from that of non-lamnids, and the combined scaling equation for all sharks examined has a slope of 1. As reviewed by Webb (1978) and Videler (1993), drag on a swimming fish is determined mainly by velocity and wetted surface area. Considering that the wetted surface area of the shark (i.e. the skin) scales with total body surface area, the principal effect of body growth on swimming power requirements are cruising speed (usually a function of *FL*) and surface area ( $M^{0.67}$ ). Therefore, the most conservative interpretation to make of an RM scaling coefficient of  $M^1$  is that, over the size range of makos examined, mass-proportional increases in TRMM would be more than adequate to power cruise swimming. However, we do not know how RM scaling or the scaling of several morphological features (e.g. body cross-sectional area, paired-fin lift area, caudal fin area) affecting drag, lift or the minimum sustainable velocity (i.e. the minimum velocity required for hydrostatic equilibrium and for ram gill ventilation) might vary across the entire size range of the mako [maximum total length, 400 cm (Compagno, 1998); 2001 International Game Fish Association recorded maximum mass, 554 kg] or that of other species we studied. We therefore cannot rule out the possibility of a change in RM scaling in larger makos or other lamnids. Carey et al. (1985), for example, reported a TRMM of approximately 3% of body mass for a small (approximately 200 kg) white shark (*Carcharodon carcharias*) but a TRMM of 6% of body mass in a much larger (1256 kg) specimen (Table 1). [Carey et al. (1985) expressed their TRMM data as a percentage of total axial muscle mass, which is here converted to percent total body mass.]

Thus, more RM scaling data and information about the scaling of factors influencing the biomechanics and physiology of high performance are needed to determine whether RM scaling differs in sharks with different RM distribution patterns. RM scaling differences in tuna and non-tuna scombrids have been attributed to the positive effect of temperature on RM function (Graham et al., 1983). Studies of mako endothermy have also raised the possibility of a physiological influence on RM scaling based on the finding that, by having a warmer RM, larger makos achieve a disproportionately greater power production per unit tissue mass (Bernal et al., 2001b, 2003).

*Oxygen delivery to RM*

Animals having a high aerobic scope usually also possess cardiorespiratory adaptations favoring high O<sub>2</sub> delivery to the working tissues. Compared with other fishes, tunas have both a high metabolic rate and a high O<sub>2</sub> transport capacity (Lowe et al., 2000; Brill and Bushnell, 2001; Korsmeyer and Dewar, 2001). Tuna RM is also relatively specialized for a high O<sub>2</sub> flux rate, having small diameter RM fibers with a high [Mb] and a rich supply of capillaries characterized by structural modifications (e.g. manifolds) that optimize O<sub>2</sub> transfer by maximizing the fiber–capillary contact area and extending red cell residence time (Mathieu-Costello et al., 1992, 1995, 1996; Dickson, 1996).

The mako shark also has numerous morphological and physiological attributes consistent with a high rate of O<sub>2</sub> delivery to its tissues (Bernal et al., 2001a), and initial studies indicate a high metabolic rate and high tissue aerobic capacity compared with other sharks (Graham et al., 1990; Dickson et al., 1993). Our study of the mako has also confirmed specializations related to a greater RM O<sub>2</sub> flux.

*RM [Mb]*

Myoglobin facilitates the diffusion of O<sub>2</sub> from a capillary to its site of utilization within the mitochondria; a larger [Mb] is thus indicative of a greater potential for O<sub>2</sub> flux (Wittenberg, 1970; Sidell, 1998; Suzuki and Imai, 1998). The finding of a high RM [Mb] in the mako, salmon and thresher sharks indicates that RM in all three species is poised for elevated O<sub>2</sub> transfer. Moreover, the RM [Mb] of these sharks is much higher than reported for other sharks (Table 2) and exceeds values reported for most other fishes except tunas (Dickson, 1996; Table 2). Our data do not show a significant scaling for RM [Mb] in either the mako or thresher sharks (Table 2) and we therefore have no new insight concerning the postulated role of intracellular [Mb] in compensating for size-related changes in blood circulation time (reviewed in Kayar et al., 1994; Goolish, 1995).

*RM ultrastructure*

RM ultrastructure was examined in only two relatively small (9.7–12 kg) mako sharks. Even though there was little difference between these sharks, our data are not adequate to fully describe mako RM ultrastructural properties or to make definitive comparisons with other species. The finding of collapsed capillaries and remaining erythrocytes in some of the RM transverse blocks moreover indicates an incomplete *in vivo* perfusion-fixation in some cases, meaning that  $Q_A(0)$ ,  $Q_A(\pi/2)$  and  $N_{CAF}$  were probably underestimated. Nevertheless, because this is the first ultrastructure information reported for a lamnid shark, a general comparison of mako RM with that of other species is warranted. Only limited comparisons are possible because of the paucity of comparative information and because important details such as specimen body mass and the sarcomere length ( $l_0$ ) at which fiber data were obtained are usually not reported. It is critically important to indicate  $l_0$

because the state of muscle contraction affects both fiber cross-sectional area and fiber diameter estimates (Mathieu-Costello and Hepple, 2002).

Mako RM fiber cross-sectional areas (at  $l_0=2.06\ \mu\text{m}$ ) are similar to those reported for other sharks (Table 3). However, mako RM capillary density [ $Q_A(0)=831\ \text{mm}^{-2}$ ] and capillary-to-fiber ratio [ $N_N(c,f)=1.19$ ], which are the highest measured for any shark species (Table 3), do indicate a greater O<sub>2</sub> diffusion capacity. Also, the mako RM capillary orientation coefficient [ $c(K,0)=1.19$ ] indicates a 19% increase in capillary length of contact per volume of muscle fiber [ $J_V(c,f)=1092\ \text{mm}^{-2}$ ] than would occur if the capillaries were straight and unbranched (Mathieu-Costello et al., 1992). While our data for mako RM ultrastructure identify features related to an increased O<sub>2</sub> flux capacity relative to other sharks, Table 3 indicates that these vascular specializations are much less extensive than those in tunas.

Mathieu-Costello et al. (1992) reported the presence of capillary manifolds in tuna locomotor muscle and suggested that these facilitated O<sub>2</sub> diffusion by increasing the capillary–fiber contact area. Capillary manifolds, which are most frequently found at the venular end of the vessel bed, also occur in the locomotor muscle of active birds (Mathieu-Costello et al., 1992). Birds and most fishes are similar in having nucleated erythrocytes and, because these are both larger and less deformable than non-nucleated erythrocytes, a possible role for capillary manifolds in enhancing red cell flow was suggested (Mathieu-Costello et al., 1992).

In view of the proposed role of manifolds in augmenting circulation, we expected to find large numbers of these structures in mako RM. In addition, with shark erythrocyte diameters averaging about 4× higher than those of tunas (Emery, 1986; Bernal et al., 2001a) and because our study (Table 3) indicates that mako RM capillary diameter is about 2× larger than in tunas, we predicted that mako manifolds would be larger.

Capillary manifolds were neither obvious nor abundant in mako RM. Fig. 3A shows what appears to be a capillary manifold in a longitudinal RM section, but this structure is much smaller than tuna manifolds (Mathieu-Costello et al., 1992), which is inconsistent with the supposed function of facilitating the flow of larger, less compliant red cells. However, we studied a limited number of longitudinal RM sections from which manifolds could be documented, and additional studies are needed to verify the presence of manifolds in makos and to search for them in larger specimens, other lamnids and other active sharks. It could be that differences between tunas and makos insofar as manifolds are concerned reflect differences in absolute RM O<sub>2</sub> demand; while the metabolic rate of a swimming mako is higher than that of other sharks, it is about 4× less than that of a tuna (Graham et al., 1990; Bernal et al., 2001a; Korsmeyer and Dewar, 2001).

Mako RM total mitochondrial volume density is 25–29%, which is in the range of other sharks and tunas (Table 3). As reviewed by Mathieu-Costello et al. (1992), conformance in mitochondrial volume density among most fishes is generally

regarded as indicating the maximum amount of non-contractile elements that can be contained within the myofibril without affecting muscle contractility (Block, 1991; Ballantyne, 1995).

In summary, lamnid–tuna evolutionary convergence in specializations for high-performance swimming extends to similarities in RM position but not in RM amount, which for tunas is larger, more variable and scales negatively with body mass in some species. All sharks in this study had 2–3% TRMM and, irrespective of RM position, had an RM scaling coefficient of 1. Similarities in tuna and lamnid RM position have a basis in similar swimming biomechanics and may also relate to the presence of regional endothermy. The common thresher shark has an RM distribution similar to that of the mako. Tuna and lamnid RM is similar in having specializations enhancing O<sub>2</sub> delivery to the mitochondria, including a high [Mb], large capillary-to-fiber ratios and structural modifications increasing capillary–fiber contact, and both groups have similar myofibrillar mitochondrial densities. Tuna RM, however, appears to have a greater degree of ‘specializations for O<sub>2</sub> delivery’, as evidenced, for example, by higher capillary density, a more extensive capillary manifold system and higher capillary tortuosity. Nonetheless, relative to other sharks, lamnids have many of the adaptations that may allow for a higher O<sub>2</sub> flux to the RM, which can potentially increase the aerobic capacity of this tissue. Additional studies comparing the RM morphology, vascularization and ultrastructure of other actively swimming ectothermic sharks are needed to understand the degree of lamnid RM morphological specializations that support their categorization as high-performance swimmers.

#### List of symbols

$\bar{a}(f)$	mean fiber cross-sectional area
$c(K,0)$	capillary orientation coefficient
$\bar{d}(c)$	mean capillary diameter
$\bar{d}(f)$	mean fiber diameter
$J_V(c,f)$	total capillary length per volume of muscle fiber
$K$	capillary anisotropy concentration parameter
$l_0$	sarcomere length
$N_{CAF}$	number of capillaries surrounding each muscle fiber
$N_N(c,f)$	capillary-to-fiber ratio
$Q_A(0)$	capillary density per mm <sup>2</sup> transverse sectional area of muscle fiber
$Q_A(\pi/2)$	capillary density per mm <sup>2</sup> longitudinal sectional area of muscle fiber
$V_V(mt,f)$	total volume density of mitochondria

We are grateful to Drs K. Dickson, N. Holland, R. Rosenblatt and R. Shadwick for critically reviewing early drafts of this manuscript. We also thank two anonymous reviewers for their suggestions. This study could not have been possible without the help for specimen collection by the captain and crew of the Research Vessels *David Starr Jordan*, *Gordon Sproul*, *Mako*, *Yellowfin* and *Splunky I*, the Fishing

Vessels *Legend*, *Sharktagger* and *Korean Limits* and the logistical support of the kind people at Chesapeake Fish Co., Sal Randazzo, Sal Mejia and Nick Vitalich, Jr, and Kent Williams of New FishHall Bait Company. We are indebted to C. Brown, E. Baner, G. Bergsma, G. Bernal, C. Brown, C. Hayleman, R. Hodges, J. Isaacs, A. Jarette, G. Lo, S. Maistro, S. Miller, C. Parinello, B. Simmons and S. Wagner for assistance with the data collection on muscle morphology. Special thanks are due to H. Lee, N. Carter, C. Chan, J. Donley, H. Dowis, S. Kanatous, C. Li, M. Trejo-Morales and J. Yan for invaluable help in data collection and analysis and to J. Valdez for logistical assistance. Support for D.B. was through the U.C. San Diego Fellowship and an NSF Graduate Fellowship. C.S. was supported by the Scripps Institution of Oceanography (SIO Directors Office and the Birch Aquarium at SIO). This work was partially supported by NSF IBN 9607699, NSF IBN 0077502 and by the University of California San Diego Academic Senate.

#### References

- Allen, G. R. (1997). *Marine Fishes of the Great Barrier Reef and South-East Asia*. Perth: Western Australia Museum.
- Altringham, J. D. and Block, B. A. (1997). Why do tuna maintain elevated slow muscle temperatures? Power output of muscle isolated from endothermic and ectothermic fish. *J. Exp. Biol.* **200**, 2617–2627.
- Altringham, J. D. and Shadwick, R. E. (2001). Swimming and muscle function. In *Fish Physiology*, vol. XIX (ed. B. A. Block and E. D. Stevens), pp. 313–344. San Diego: Academic Press.
- Anderson, S. A. and Goldman, K. J. (2001). Temperature measurements from salmon sharks, *Lamna ditropis*, in Alaskan waters. *Copeia* **2001**, 794–796.
- Ballantyne, J. S. (1995). Metabolic organization of thermogenic tissues of fishes. In *Biochemistry and Molecular Biology of Fishes*, vol. 4 (ed. P. W. Hochachka and T. Mommsen), pp. 241–257. Amsterdam: Elsevier Science.
- Bernal, D., Dickson, K. A., Shadwick, R. E. and Graham, J. B. (2001a). Analysis of the evolutionary convergence for high performance swimming in lamnid sharks and tunas. *Comp. Biochem. Physiol.* **129A**, 695–726.
- Bernal, D., Sepulveda, C. and Graham, J. B. (2001b). Water-tunnel studies of heat balance in swimming mako sharks. *J. Exp. Biol.* **204**, 4043–4054.
- Bernal, D., Smith, D., Lopez, G., Weitz, D., Grimmering, T., A., D. K. and Graham, J. B. (2003). Comparative studies of high performance swimming in sharks. II. Metabolic biochemistry of locomotor and myocardial muscle in endothermic and ectothermic sharks. *J. Exp. Biol.* **206**, 2845–2857.
- Block, B. A. (1991). Evolutionary novelties: how fish have built a heater out of muscle. *Am. Zool.* **31**, 726–742.
- Block, B. A. and Finnerty, J. R. (1994). Endothermy in fishes: a phylogenetic analysis of constraints, predispositions, and selection pressures. *Env. Biol. Fish.* **40**, 283–302.
- Bone, Q. (1978a). Locomotor muscle. In *Fish Physiology*, vol. VII (ed. W. S. Hoar and D. J. Randall), pp. 361–417. New York: Academic Press.
- Bone, Q. (1978b). Myotomal muscle fiber types in *Scomber* and *Katsuwonus*. In *The Physiological Ecology of Tunas* (ed. G. D. Sharp and A. E. Dizon), pp. 183–205. New York: Academic Press.
- Bone, Q. and Chubb, A. D. (1983). The retial system of the locomotor muscle in the thresher shark. *J. Mar. Biol. Assoc. UK* **63**, 239–241.
- Brill, R. W. (1996). Selective advantages conferred by the high performance physiology of tunas, billfishes, and dolphin fish. *Comp. Biochem. Physiol.* **A 113**, 3–15.
- Brill, R. W. and Bushnell, P. G. (2001). The cardiovascular system of tunas. In *Fish Physiology*, vol. XIX (ed. B. A. Block and E. D. Stevens), pp. 79–120. San Diego: Academic Press.
- Carey, F. G., Casey, J. G., Pratt, H. L., Urquhart, D. and McCosker, J. E. (1985). Temperature, heat production and heat exchange in lamnid sharks. *Mem. Southern Calif. Acad. Sci.* **9**, 92–108.
- Carey, F. G. and Teal, J. M. (1966). Heat conservation in tuna fish muscle. *Proc. Natl. Acad. Sci. USA* **56**, 1464–1469.

- Carey, F. G. and Teal, J. M. (1969a). Mako and porbeagle: warm bodied sharks. *Comp. Biochem. Physiol.* **28**, 199-204.
- Carey, F. G. and Teal, J. M. (1969b). Regulation of body temperature by the bluefin tuna. *Comp. Biochem. Physiol.* **28**, 205-213.
- Carey, F. G., Teal, J. M., Kanwisher, J. W. and Lawson, K. D. (1971). Warm bodied fish. *Am. Zool.* **11**, 135-145.
- Compagno, L. J. V. (1998). Lamnidae. Mackerel sharks, makos, white sharks, porbeagles. In *FAO Identification Guide For Fishery Purposes. The Living Marine Resources of the Western Central Pacific* (ed. K. E. Carpenter and V. H. Niem), pp. 1274-1278. Rome: FAO.
- Dickson, K. A. (1995). Unique adaptations of the metabolic biochemistry of tunas and billfishes for life in the pelagic environment. *Env. Biol. Fish.* **42**, 65-97.
- Dickson, K. A. (1996). Locomotor muscle of high performance fishes: what do comparisons of tunas with other ectothermic taxa reveal? *Comp. Biochem. Physiol. A* **113**, 39-49.
- Dickson, K. A., Gregorio, M. O., Gruber, S. J., Loeffler, K. L., Tran, M. and Terrel, C. (1993). Biochemical indices of aerobic and anaerobic capacity in muscle tissues of California elasmobranch fishes differing in typical activity level. *Mar. Biol.* **117**, 185-193.
- Emery, S. H. (1986). Hematological comparisons of endothermic vs ectothermic elasmobranch fishes. *Copeia* **1986**, 700-705.
- Froese, R. and Pauly, D. (ed.) (2002). *FishBase*. World Wide Web electronic publication. www.fishbase.org.
- Goodson, G. (1988). *Fishes of the Pacific Coast. Alaska to Peru, including the Gulf of California and the Galapagos Islands*. Stanford, Stanford University Press.
- Goolish, E. M. (1989). The scaling of aerobic and anaerobic muscle power in rainbow trout, *Salmo gairdneri*. *J. Exp. Biol.* **147**, 493-505.
- Goolish, E. M. (1995). The metabolic consequences of body size. In *Biochemistry and Molecular Biology of Fishes*, vol. IV (ed. P. W. Hochachka and T. Mommsen), pp. 335-366. Amsterdam: Elsevier Science.
- Graham, J. B., Dewar, H., Lai, N. C., Lowell, W. R. and Arce, S. M. (1990). Aspects of shark swimming performance determined using a large water tunnel. *J. Exp. Biol.* **151**, 175-192.
- Graham, J. B. and Dickson, K. A. (2000). The evolution of thunniform locomotion and heat conservation in scombrid fishes: new insights based on the morphology of *Allothunnus fallai*. *Zool. J. Linn. Soc. Lond.* **129**, 419-466.
- Graham, J. B. and Dickson, K. A. (2001). Anatomical and physiological specializations for endothermy. In *Fish Physiology*, vol. XIX (ed. B. A. Block and E. D. Stevens), pp. 121-165. San Diego: Academic Press.
- Graham, J. B., Koehn, F. J. and Dickson, K. A. (1983). Distribution and relative proportions of red muscle in scombrid fishes: consequences of body size and relationships to locomotion and endothermy. *Can. J. Zool.* **61**, 2087-2096.
- Greer-Walker, M. and Pull, G. (1975). A survey of red and white muscle in marine fish. *J. Fish. Biol.* **7**, 295-300.
- Gruber, S. H. and Compagno, L. J. V. (1981). Taxonomic status and biology of the bigeye thresher, *Alopias superciliosus* (Lowe, 1839). *Fish. Bull. US Nat. Mar. Fish. Serv.* **79**, 617-640.
- Gubanov, Y. P. (1972). On the biology of the thresher shark (*Alopias vulpinus*, Bonaterre) in the northwest Indian Ocean. *J. Ichthyol.* **12**, 591-600.
- Johnston, I. A. and Brill, R. W. (1984). Thermal dependence of contractile properties of single skinned muscle fibers from Antarctic and various warm water marine fishes including skipjack tuna (*Katsuwonus pelamis*) and kawakawa (*Euthynnus affinis*). *J. Comp. Physiol. B* **155**, 63-70.
- Katz, S. L. (2002). Design of heterothermic muscle in fish. *J. Exp. Biol.* **205**, 2251-2266.
- Katz, S. L., Syme, D. A. and Shadwick, R. E. (2001). High-speed swimming. Enhanced power in yellowfin tuna. *Nature* **410**, 770-771.
- Kayar, S. R., Hoppeler, H., Jones, J. H., Longworth, K., Armstrong, R. B., Laughlin, M. H., Lindstedt, S. L., Bicudo, J. E. P. W., Groebe, K. and Weibel, E. R. (1994). Capillary blood transit time in muscles in relation to body size and aerobic capacity. *J. Exp. Biol.* **194**, 69-81.
- Kohler, N. E., Casey, J. G. and Turner, P. A. (1994). Length-weight relationships for 13 species of sharks from the western North Atlantic. *US Fish. Bull.* **93**, 412-418.
- Korsmeyer, K. E. and Dewar, H. (2001). Tuna metabolism and energetics. In *Fish Physiology*, vol. XIX (ed. B. A. Block and E. D. Stevens), pp. 35-78. San Diego: Academic Press.
- Kryvi, H., Flatmark, T. and Totland, G. K. (1981). The myoglobin content in red, intermediate and white fibers of the swimming muscles in three species of shark – a comparative study using high-performance liquid chromatography. *J. Fish. Biol.* **18**, 331-338.
- Lai, N. C., Korsmeyer, K. E., Katz, S., Holts, D. B., Laughlin, L. M. and Graham, J. B. (1997). Hemodynamics and blood properties of the shortfin mako shark (*Isurus oxyrinchus*). *Copeia* **1997**, 424-428.
- Last, P. R. and Stevens, J. D. (1994) *Sharks and Rays of Australia*. Melbourne: CSIRO.
- Lindsey, C. C. (1978). Form, function, and locomotory habits in fish. In *Fish Physiology*, vol. VII (ed. W. S. Hoar and D. J. Randall), pp. 1-100. New York: Academic Press.
- Lowe, T. E., Brill, R. W. and Cousins, K. L. (2000). Blood oxygen-binding characteristics of bigeye tuna (*Thunnus obesus*), a high-energy-demand teleost that is tolerant to low ambient oxygen. *Mar. Biol.* **136**, 1087-1098.
- Mathieu, O., Cruz-Orive, L. M., Hoppeler, H. and Weibel, E. R. (1983). Estimating length density and quantifying anisotropy in skeletal muscle capillaries. *J. Microsc.* **131**, 131-146.
- Mathieu-Costello, O., Agey, P. J. and Logemann, R. B. (1992). Capillary-fiber geometrical relationships in tuna red muscle. *Can. J. Zool.* **70**, 1218-1229.
- Mathieu-Costello, O., Brill, R. W. and Hochachka, P. W. (1995). Design for a high speed path for oxygen: tuna red muscle ultrastructure and vascularization. In *Biochemistry and Molecular Biology of Fishes*, vol. IV (ed. P. W. Hochachka and T. Mommsen), pp. 1-13. Amsterdam: Elsevier Science.
- Mathieu-Costello, O., Brill, R. W. and Hochachka, P. W. (1996). Structural basis for oxygen delivery: muscle capillaries and manifolds in tuna red muscle. *Comp. Biochem. Physiol. A* **113**, 25-31.
- Mathieu-Costello, O. and Hepple, R. T. (2002). Muscle structural capacity for oxygen flux from capillary to fiber mitochondria. *Exerc. Sport Sci. Rev.* **30**, 80-84.
- Mollet, H. F. and Cailliet, G. M. (1996). Using allometry to predict body mass from linear measurements of the white shark. In *Great White Sharks: The Biology of Carcharodon carcharias* (ed. A. P. Klimley and D. G. Ainley), pp. 81-90. San Diego: Academic Press.
- Moyes, C. D., Mathieu-Costello, O., Brill, R. W. and Hochachka, P. W. (1992). Mitochondrial metabolism of cardiac and skeletal muscles from a fast, *Katsuwonus pelamis*, and slow, *Cyprinus carpio*, fish. *Can. J. Zool.* **70**, 1246-1253.
- Reif, W.-E. and Weishampel, D. B. (1986). Anatomy and mechanics of the lunate tail in lamnid sharks. *Zool. Jb. Anat.* **114**, 221-234.
- Sfakiotakis, M., Lane, D. M. and Davies, B. C. (1999). Review of fish swimming modes for aquatic locomotion. *IEEE J. Oceanic Eng.* **24**, 237-252.
- Shadwick, R. E., Katz, S. L., Korsmeyer, K. E., Knower, T. and Covell, J. W. (1999). Muscle dynamics in skipjack tuna: timing of red muscle shortening in relation to activation and body curvature in steady swimming. *J. Exp. Biol.* **202**, 2139-2150.
- Sidell, B. D. (1998). Intracellular oxygen diffusion: the roles of myoglobin and lipid at cold body temperature. *J. Exp. Biol.* **201**, 1118-1127.
- Suzuki, T. and Imai, K. (1998). Evolution of myoglobin. *Cell. Mol. Life Sci.* **54**, 979-1004.
- Tricas, T. C., Deacon, K., Last, P., McCosker, J. E., Walker, T. I. and Taylor, L. (1997). *Sharks and Rays*. Sydney: Weldon Owen.
- Totland, G. K., Kryvi, H., Bone, Q. and Flood, P. R. (1981). Vascularization of the lateral muscle of some elasmobranchimorph fishes. *J. Fish Biol.* **18**, 223-234.
- Videler, J. J. (1993). *Fish Swimming*. New York: Chapman and Hall.
- Webb, P. W. (1978). Hydrodynamics: nonscombriform fish. In *Fish Physiology*, vol. VII (ed. W. S. Hoar and D. J. Randall), pp. 189-237. New York: Academic Press.
- White, F. C., Kelly, R., Kemper, S., Schumacker, P. T., Gallagher, K. R. and Laurs, R. M. (1988). Organ blood flow, haemodynamics, and metabolism of the albacore tuna *Thunnus alalunga* (Bonaterre). *Exp. Biol.* **47**, 161-169.
- Wittenberg, J. B. (1970). Myoglobin-facilitated oxygen diffusion: role of myoglobin in oxygen entry into muscle. *Physiol. Rev.* **50**, 559-636.